Ice sheet extent and early deglacial history of the southwestern sector of the Greenland Ice Sheet

David H. Roberts[a,*], Antony J. Long[a], Christoph Schnabel[b], Bethan J. Davies[a], Sheng Xu[b], Matthew J.R. Simpson[c], Phillipe Huybrechts[d]

[a]Department of Geography, Durham University, Science Laboratories, South Road, Durham, DH1 3LE, United Kingdom
[b]NERC Cosmogenic Isotope Analysis Facility, Scottish Universities Environmental Research Centre, Scottish Enterprise Technology Park, East Kilbride, G75 0QF, United Kingdom
[c] Department of Earth Sciences, Durham University, Science Laboratories, South Road, Durham, DH1 3LE, United Kingdom
[d] Vrije Universiteit Brussel, Earth System Sciences & Department of Geography, Pleinlaan 2, B-1050 Brussels, Belgium

[*]Corresponding author. Tel: 0044-191-344-1935; Fax: 0044-191-334-1801.
Email: D.H.Roberts@durham.ac.uk (D.H.Roberts).

Abstract

The offshore and coastal geomorphology of southwest Greenland records evidence for the advance and decay of the Greenland Ice Sheet during the Last Glacial Maximum. Regional ice flow patterns in the vicinity of Sisimiut show an enlarged ice sheet that extended southwestwards on to the shelf, with an ice stream centred over Holsteinsborg dyb. High level periglacial terrain composed of blockfield and tors is dated to between 101 – 142 ka using ^{26}Al and ^{10}Be cosmogenic exposure ages. These limit the maximum surface elevation of the Last Glacial Maximum ice sheet in this part of southwest Greenland to ca 750 – 810 m asl, and demonstrate that terrain above this level has been ice free since MIS 6. Last Glacial Maximum ice thickness on the coast of ca 700 m implies that the ice sheet reached the mid to outer continental shelf edge to form the Outer Hellefisk moraines. Exposure dates record ice surface thinning from 21.0 to 9.8 ka, with downwasting rates varying from 0.06 to 0.12m yr^{-1}. This reflects strong surface ablation associated with increased air temperatures running up to the Bølling Interstadial (GIS1e) at ca 14 ka, and later marine calving under high sea levels. The relatively late retreat of the Itilleq ice stream inland of the present coastline is similar to the pattern observed at Jakobshavn Isbræ, located 250 km north in Disko Bugt, which also retreated from the continental shelf after ca 10 ka. We hypothesise that the ice streams of West Greenland persisted on the inner shelf until the early Holocene because of their considerable ice thickness and greater ice discharge compared with the adjacent ice sheet.

1.0 Introduction

Mass balance observations of the Greenland Ice Sheet (GIS) show that it is undergoing rapid change (Howat *et al*., 2005; Chen *et al*., 2006; Joughin, 2006; Rignot and Kanagaratnam, 2006; Velicogna and Wahr, 2006; Holland *et al*., 2008). These short term changes may be a response to climate warming, or natural instability in ice sheet behaviour. There is a need, therefore, to develop longer-term perspectives on ice sheet

behaviour in order to improve our knowledge of the internal and external environmental controls that drive ice sheet fluctuation.

Furthering our understanding the long term behaviour of the western sector of the GIS is important for several reasons. Firstly, early geomorphological research established the Sisimiut region as a benchmark study area for the deglacial chronology of West Greenland (Weidick, 1972; Ten Brink and Weidick, 1975; Kelly, 1985; Funder, 1989). However, the deglacial chronology relied largely on radiocarbon dated marine shells and direct dating of deglacial terrain was not possible. Moreover, recent work has begun to challenge aspects of the resulting regional deglacial chronology. In the Disko Bugt region, for example, ice margin retreat occurred later than originally thought, whilst the early Holocene "Fjord stade" moraines, previously dated to ca 8 kcal. yr BP, are now shown to vary in age between 10 - 8 kcal. yr BP, their formation controlled by the interplay between topography and ice sheet dynamics, and not just climate (Long and Roberts, 2002; Long *et al.,* 2006). Secondly, the area has been the focus of regional scale ice sheet modelling, but this been poorly constrained chronologically and geologically (Van Tatenhove *et al*., 1996; Tarasov and Peltier, 2002; Simpson *et al.,* 2009). Thirdly, although the Last Glacial Maximum (LGM) dynamics of this sector of the ice sheet were heavily influenced by shelf-based coalescent ice stream systems, little is known of their history (Long and Roberts; 2003; Roberts and Long, 2005; Weidick and Bennike, 2007; Roberts *et al.,* submitted) (Fig. 1). Lastly, today the ice sheet here has a low gradient surface profile and so experiences rapid changes in mass balance due to air temperature change (Box *et al*., 2006). The region is also sensitive to changes in ocean temperature, with the relatively warm West Greenland Current driving Holocene and more recent ice margin instabilities (Lloyd, 2006; Holland *et al*., 2008).

This research aims to establish the LGM history of the southwestern sector of the GIS in the vicinity of Itilleq, south of Sisimiut, a previously unexplored area that provides the opportunity to investigate; local and regional patterns of ice flow fed from local outlet glaciers and the main ice sheet; ice stream activity along the southwest coast; LGM maximum ice sheet ice thickness and pre-LGM landscape evolution. Through the application of geomorphological mapping and cosmogenic radionuclide exposure (CRN) dating we develop a new record of ice sheet dimension and deglacial history. This work forms part of a wider programme of research concerned with reconstructing the Late Quaternary history of the GIS using relative sea-level data (Long and Roberts, 2002, 2003; Long *et al*, 1999, 2003, 2006, 2008) coupled with CRN dating of deglaciated terrain (Sparrenbom *et al*., 2006; Håkansson *et al*., 2007, 2008; Kelly *et al*., 2008; Roberts *et al*., 2008; Rinterknecht *et al.,* 2009;).

2.0 The Late Quaternary glacial history of West Greenland

The oldest glacial deposits in West Greenland belong to the Fiskebanke glaciation (MIS 6; 130 ka BP), and comprise partially preserved, deeply weathered tills and erratics found on coastal mountains (Kelly, 1985; Funder, 1989), although they have not been directly dated. The LGM in Greenland is known as the Sisimiut Stade (Funder, 1989), with maximum ice thickness of ca 700 and 1000 m asl in the Sisimiut region inferred from trimlines, block field and tors (Kelly, 1985) (Fig. 2). Kelly (1985) argues that the elevation of these landforms imply a relatively thin LGM ice sheet, which just reached the shelf and formed the Inner Hellefisk moraines (Fig. 1) (Brett and Zarudzki, 1979; Funder, 1989). Some support for this is provided by recently published cosmogenic dates to north of Sisimiut, which suggest LGM ice surface did not exceed 500 to 840 m

asl (Rinterknecht *et al.,* 2009). This 'small ice' model contrasts with recent research in the southern part of the GIS, where Bennike *et al.* (2002) and Weidick *et al.* (2004) suggest ice 1500 m thick covered the coastal mountains during the LGM and extended offshore to the shelf edge. This is further supported by recent sea level studies by Sparrenbom *et al*. (2006) from the Nanortalik region which also suggests extensive ice cover across the continental shelf.

The offshore bathymetry of West Greenland shows several large troughs that run northeast to southwest across the shelf and terminate in trough mouth fans (Fig. 1; Brett and Zarudski, 1979). Several authors have suggested they have pre-glacial origins as Late Pliocene/Early Quaternary fluvial systems (e.g. Sommerhof, 1975), though their morphology is principally controlled by the structure of the Precambrian basement rocks and recent exploitation by glacial activity (Fig. 1), most likely by large ice streams (Roberts and Long, 2005; Weidick and Bennike, 2007).

Existing models suggest that in West Greenland ice sheet retreat following the LGM began with the break-up of the marine-based portion of the ice sheet sometime between ca 15 and 10 kcal. yr BP (Funder and Hansen, 1996), although others propose later deglaciation between 13 and 11.5 kcal. yr BP (Ingolfsson *et al*., 1990; Weidick, 1996). The earliest dated marine shells in the Sisimiut area point to ice free conditions on the outer coast after ca 10.4 to 10.2 kcal. yr BP (Weidick, 1972; Kelly, 1973, 1979; Bennike and Björck, 2002). This was followed by a slower retreat of the land-based ice during the early Holocene, with moraines marking temporary marginal positions (Ten Brink and Weidick, 1975; Funder and Hansen, 1996; van Tatenhove *et al.*, 1996; Long *et al.,* 2006). In the Sisimiut – Søndre Strømfjord region, van Tatenhove *et al.* (1996) report up to six moraine belts between the coast and the present margin with the earliest dated to 12.3 kcal. yr BP.

This paper firstly considers geomorphological evidence to constrain LGM ice sheet behaviour and thickness in the Itilleq region of southwest Greenland, south of Sisimiut, dating both glacial and periglacial landscapes using CRN dating techniques. It then establishes the timing of deglaciation, rates of ice surface thinning and the nature of ice margin retreat. Finally, we compare the results of this study with other records from elsewhere in West Greenland and consider the driving mechanisms behind ice sheet decay at the end of the LGM.

2.1 Study site

The Itilleq area lies on the coast to the west of Søndre Strømfjord, ca 200 km to the west of the present GIS margin. The area has been dissected over multiple glacial cycles by southwest flowing outlet glaciers and ice streams (Fig. 3). To the northeast and southeast, deep troughs (Nordre Isortoq; Søndre Strømfjord) dissect the landscape and the mountains reach elevations up to 1500 m asl. These areas of high terrain support trimlines, blockfield and tors above glaciated terrain (Kelly, 1985). The bedrock geology of the study area is Precambrian Archaen gneiss to the south with Palaeoproterozoic rocks to the north. This alkaline province includes swarms of alkaline ultramafic dykes (Larsen, 1991). The foliation and dyke swarms exhibit a strong ENE/WSW trend.

Ice sourced from the main ice sheet flowed along Itilleq, Kangerluarsuk and Ikertooq fjords during glacial periods, converging on the coast between Sisimiut and Itilleq. The

offshore bathymetry to the west of the field area reveals a large trough trending northeast to southwest (Holsteinsborg dyb, > 600m deep), which acted as a potential ice stream pathway (Fig. 1; Roberts *et al*., submitted). The coastal fringe to the west of the Nattoralinnguaq valley study area is a low-lying strandflat, composed of glacially scoured terrain and rarely rising above 100 m asl. East of this the landscape rises steeply into a mountainous alpine terrain (1000-2000 m asl) situated to the west of Sukkertoppen ice cap (Fig. 3). The Nattoralinnguaq valley is bounded north and south by steep valley walls dissected by small cirque glaciers. To the east it is partially blind and backed by steep headwalls occupied by a small cirque glacier.

3.0 Methodology

3.1 Field mapping

Glacial landforms were mapped in a corridor from the present coast along the areas bordering the Nattoralinnguaq valley (Figs. 3 and 4). Base maps were established using 1:150,000 scale aerial photographs. These were ground-truthed and supplemented by extensive field mapping. Abraded bedrock, roche moutonnées and striae were mapped in order to reconstruct basal ice flow patterns using established criteria for the identification of subglacial erosional features (Gordon, 1981; Glasser and Warren, 1990; Sugden *et al*., 1992; Roberts and Long, 2005). Recessional moraines were mapped in Nattoralinnguaq valley in order to establish the nature and timing of ice retreat at low elevations, below the local marine limit (ca 140 m asl; Ten Brink and Weidick, 1975; Long *et al*., 2009).

Trimlines were identified as limits separating glacially eroded terrain from shattered periglacial blockfield areas (Kelly, 1985; Ballantyne, 1997). To test whether trimlines represented former ice sheet surface altitudes, englacial thermal boundaries (with upper blockfields being protected by cold ice) or post glacial weathering limits, samples were collected for CRN dating to establish exposure and burial histories (e.g. Bierman *et al*., 1999; Marsella *et al*., 2000). Altitudes are expressed in metres above present sea level (asl) with a precision of ± 10 m determined by a handheld GPS.

3.2 Surface radionuclide (CRN) exposure dating

Samples for CRN dating were collected from intact bedrock surfaces and large subglacial erratics (typically >2 m^3) from two sampling profiles across the western edge of the Nattoralinnguaq valley (Fig. 5). All the samples comprise Archaen banded quartz gneiss. Where possible, paired samples of bedrock and erratics were collected to validate erosion surface ages, and to also test for potential multi-event erratic histories. We avoided sites that were potentially affected by snow or sediment cover and sampled rock that demonstrated no (or very limited) evidence for surficial weathering. Samples were taken using a rock cutting saw that allowed blocks (10 cm x 10 cm x 4 cm) to be removed at least 30 cm from all edges. At each location sample position, altitude, dimension, surface characteristics, direction of dip and topographic shielding were recorded. Data regarding sample density, geographic scaling, and thickness attenuation are given in Table 1.

The samples were collected from areas adjacent to and within the Nattoralinnguaq valley to determine the rate of ice down-wasting and marginal retreat (Fig. 5). The samples cover an altitudinal range from 120 - 850 m asl and include samples collected

from above and below local trimlines, in blockfield and glacially abraded terrains. Samples were also collected at varying vertical distances from trimlines on steep valley side locations in order to minimize potential problems with cosmogenic isotope inheritance.

3.2.1 Sample preparation

The sample preparation and $^{10}Be/^{26}Al$ measurement procedures used in this study are described in detail in Wilson *et al*. (2008) and Ballantyne *et al.* (2009). In this project ca 250 µg Be was added as a carrier per sample. Inherent Al concentrations in quartz were determined with an ICP-MS at SUERC. The relative standard uncertainty of this determination was 3%. Al carrier was added to most samples so that 2 mg Al per sample was reached.

3.2.2. ^{10}Be measurements

The $^{10}Be/^{9}Be$ ratios were measured with the 5 MV accelerator mass spectrometer at SUERC as part of a routine Be run. Measurement is described in detail in Maden *et al.* (2007). Typical ion currents of $^{9}Be^{16}O^{-}$ were 5 µA. NIST SRM4325 with a calibrated $^{10}Be/^{9}Be$ ratio of $3.06 * 10^{-11}$ was used for normalisation. The effect of this choice is discussed in detail in Roberts *et al*. (2008). The exposure ages presented here are valid even if the ^{10}Be concentrations were to be corrected according to the re-calibration of Nishiizumi *et al.* (2007). The $^{10}Be/^{9}Be$ ratios of the processing blanks prepared with the samples were $5 *10^{-15}$ and $7 * 10^{-15}$, respectively. These ratios were subtracted from the Be isotope ratios of the respective samples. Blank-corrected $^{10}Be/^{9}Be$ ratios of the samples ranged from $8.2 *10^{-14}$ to $2.6 * 10^{-12}$. The treatment of the uncertainties that contribute to the uncertainty of the ^{10}Be concentration in atoms g^{-1} quartz is described in Roberts *et al*. (2008).

3.2.3. ^{26}Al measurements

The measurement procedures at the SUERC AMS are described in detail in Maden *et al.* (2007) and Roberts *et al*. (2008). Typical ion currents of $^{27}Al^{-}$ were 400-550 nA. Z92-0222 (donated from PRIME Lab, Purdue) with a nominal $^{26}Al/^{27}Al$ ratio of $4.11 *10^{-11}$. The $^{26}Al/^{27}Al$ ratios of the processing blanks prepared with the samples was $1 *10^{-15}$ and $2 * 10^{-15}$. These ratios were subtracted from the Be isotope ratios of the respective samples. Blank-corrected $^{26}Al/^{27}Al$ ratios of the samples ranged from $1.7 *10^{-13}$ to $4.8 * 10^{-12}$. Aluminium (^{27}Al) concentrations were determined from an aliquot of the dissolved sample before carrier addition. These inherent concentrations were determined with ICP-MS SUERC (standard uncertainty: 3%). The treatment of the uncertainties that contribute to the uncertainty of the ^{26}Al concentration in atoms g^{-1} quartz is described in Roberts *et al*. (2008).

3.2.4 Exposure age calculation

Exposure ages were calculated using the CRONUS-Earth online calculator (Balco *et al*., 2008) (version: wrapper script 2.0; main calculator 2.0; constants 2.0). The Sea-level High Latitude (SLHL) production rate (spallogenic production only) used is 4.96±0.43 atoms g^{-1} yr^{-1}. The ratio of the SLHL production rate ratios for ^{10}Be and ^{26}Al is 6.1. Attenuation correction for sample thickness uses an attenuation length of 160 g cm^{-2}. Topographic shielding correction is determined according to Dunne *et al*. (1999). The

exposure ages are not corrected for past geomagnetic field variations. Including a simple palaeomagnetic correction (Nishiizumi *et al.* 1989) results in ages ca 1% older ages than presented for the samples with an exposure age of about 10 ka. For the samples that were exposed since MIS 6 corrected ages are up to 3% older but still fall within the internal uncertainty of the presented data. For ages based on ^{10}Be concentrations we also present data based on 1 * 10^{-4} cm yr^{-1} erosion rate. Age determinations include a correction for pressure related to the altitude, latitude and longitude according to the mean global surface pressure field of the NCEP-NCAR re-analysis (www.cdc.noaa.gov/ncep_reanalysis/), but assume the standard atmosphere for geographical scaling of the production rate.

The relative internal uncertainty of the exposure ages is equivalent to the relative uncertainty of the radionuclide concentration. The external uncertainty also includes the uncertainty of the production rate. Typical age uncertainties associated with the ^{10}Be dates vary between 1000 and 2500 years for the exposure ages younger than 30 ka (Table 2), although these increase significantly where ages are in excess of 100 ka. In the following discussion we refer to mean ages, and exposure dates are presented in 'ka', meaning thousand years before the date of sample collection (AD 2006). Radiocarbon dates are reported as calibrated ages (kcal. yr BP).

We use ^{10}Be and ^{26}Al analyses to test for complex exposure and shielding histories in high elevation sites above trimlines (Gosse and Phillips, 2001). Plots of our ^{26}Al/^{10}Be ratios versus ^{10}Be concentrations show that all but one of our exposure ages fall within a 2 sigma error range of the theoretical erosion island envelope, and there is approximate concordance in ^{26}Al and ^{10}Be ages (Table 2). Only Nag 11 has a low ^{26}Al/^{10}Be ratio outside a 2 sigma error range, suggesting limited bedrock erosion and CRN inheritance. Accordingly, in the following discussion we refer only to the ^{10}Be age determinations.

4.0 Results

4.1 Regional ice flow patterns and glacial geomorphology

The low lying coastal plain in the Qingartaq area is glacially abraded and bordered to the east by mountainous alpine terrain. Occasional striae and roche moutonnée long axes show an initial westerly ice movement from Nattoralinnguaq and adjacent valleys, but this is overprinted by a later southwest flow phase sourced from Itilleq fjord (Fig. 4). Ice exiting Itilleq fjord is hypothesised to have formed the southern edge of a large regional composite ice stream that flowed southwest as a consequence of ice in Kangerluarsuk and Ikertooq fjords further north being topographically captured and routed into Holsteinsborg dyb (Fig. 3, Roberts *et al*., submitted). The pattern of recessional moraines which bend southwest from the mouth of the Nattoralinnguaq valley suggests that Nattoralinnguaq ice was deflected southwestwards by the action of Itilleq fjord ice moving obliquely across the coastal plain (Fig. 4). The Qingartaq coastal plain was, thus, a zone of coalescence between the Itilleq fjord ice and local valley glaciers originating from the nearby mountains. Depositional landforms are rare along the coast, much of which lies below the local marine limit.

The Nattoralinnguaq valley and surrounding mountains have both erosional and depositional glacial features, as well as periglacial features. Above 660 m asl on the north side of Nattoralinnguaq, the steep mountain sides and upper ridges are covered in

blockfield, with densely packed, large angular blocks of local bedrock, separated by thin spreads of poorly sorted sediment and occasional poorly developed tors (Figs. 6 and 7). This is similar to the description of blockfield terrain by Kelly (1985) in mountainous terrain adjacent to Nordre Isortoq and Søndre Strømfjord. Such terrain is separated from lower-lying glacially abraded areas by a trimline on the north side of Nattoralinnguaq between 660 -700 m asl (Fig. 6). Glacially abraded terrain is ubiquitous below this level although the southern side of the valley is heavily dissected by small corries (Fig. 8). Roche moutonnée and striae long axes run east to west, sub-parallel to the Nattoralinnguaq valley axis (Fig. 4).

Below ca 150 m asl the Nattoralinnguaq valley floor is mainly characterised by a nested recessional moraine sequence and occasional marine deltas. The recessional moraines are composed of massive grey sand silt diamicts with *in situ* paired marine molluscs (eg. *Hiatella acrtica, Mya truncata*). The ridges run transverse to ice flow within the valley, but once west of the mouth of the Nattoralinnguaq, they curve around to the southwest and are unconstrained by topography (Figs 4, 9a, b). The ridges are also slope conformable within the valley, being highest on the valley edges and falling in elevation towards the valley centre. There upper limit is coincident with the local marine limit at ca 140 m asl and they fall gently in elevation down valley.They are closely and uniformly spaced being up to 100-300 m long, 10 m high, 20-30 m wide and typically 50 m apart. In some instances the moraines are on-lapped by small flat topped deltas.

The moraines have characteristics similar to recessional De Geer moraines (cf. Lindén and Möller, 2005; Heyman and Hättestrand, 2006). The grey poorly sorted diamicts with *in situ* marine fauna that lie below the local marine limit suggests they are glaciomarine in origin. Their density and uniform spacing in planform suggests they relate to a retreating grounding line controlled by calving along ice transverse crevasses, each ridge representing a small subaqueous push moraine composed of ice proximal rainout sediments (Lindén and Möller, 2005). Their overall regional geometry, with a restricted southwesterly trending tract, also suggests that ice along the coast remained in place as the Nattoralinnguaq glacier calved headward back in to its valley.

4.2 Landscape chronology

The oldest CRN dates occur above the blockfield trimline on the north side of the Nattoralinnguaq valley. Three dates (Nag 1, 2 and 4) demonstrate that this terrain, above 800 m asl, predates the LGM and became ice free between 101 – 142 ka (Fig. 5; Table 2). The concordance between our ^{10}Be and ^{26}Al dates suggest the upper ridge and summit areas adjacent to Nattoralinnguaq valley were ice free during the LGM and were not covered by cold based ice. This limits the ice sheet surface during MIS 2 to a maximum of 755 - 813 m asl and suggests that areas above ca 800 m asl have been unglaciated since the Fiskebanke glaciation (MIS 6). For such high elevation terrain (> ca 800 m asl) to have been glacially abraded and cosmogenically ‘reset’ by warm based ice during MIS 6, suggests an ice sheet surface of at least ca 1000 m asl, ca 200 m thicker than the LGM ice sheet at this locality.

The lowest vertical extent of blockfield in the study area is at ca 660 m asl, but ^{10}Be and ^{26}Al dates from Nag 3 and Nag 5 at 55.4 ± 5.2 ka and 29.5 ± 2.7 ka respectively (Fig. 5; Table 2) suggest that terrain between 660 and 755 m asl has been partially glacially eroded. The lower limit of the blockfield could be a result of postglacial downslope gelifluction. Below 660 m asl the cosmogenic exposure dates record ice thinning and ice

margin retreat between 26.7 ± 2.4 ka and 9.8 ± 0.9 ka, although the data do not show progressive thinning and there are some age reversals. Nag 6 and 7 show the ridge along the northern side of the Nattoralinnguaq valley (500-600 m asl) became ice free around 21.0 ± 1.9 ka to 20.3 ± 1.9 ka (Fig. 5; Table 2). The sequencing of ice downwasting is then somewhat confused by Nag 8 and 11 which suggest that lower elevation terrain at ca 430 - 450 m asl did not become ice free until ca 27 ± 2.4 ka. The concordance between ^{10}Be and ^{26}Al ages for Nag 8 does not suggest a complex burial or erosion history, but the lack of agreement between Nag 11 and Nag 12 (where a stoss and leeside sample pair were taken from the same roche moutonnée; Nag 11: 26.7 ± 2.4 ka/stoss-side and Nag12: 18.0 ± 1.6 ka/lee-side; Table 2), suggests the date of 26.7 ka for Nag 11 is incorrect, the leeside sample clearly being younger. There is also a clear offset in the ^{10}Be and ^{26}Al ages for Nag 11, and it's ^{26}Al/^{10}Be ratio falls outside a 2 sigma error range, suggesting limited bedrock erosion and CRN inheritance (Table 2).

Nag 9 and 10 suggest that ice thinned further to 230 m asl between 18.4 ± 1.7 ka and 16.3 ± 1.5 ka up-valley, while ages from samples along the ridge further west show ice had thinned to 309 m asl by 14.9 ± 1.3 ka (Nag 14) and to 150 m asl by 13.6 ± 1.4 ka (Nag 15; Table 2; Fig. 5). Nag 15 may well have been located in the coalescence zone between Itilleq ice stream and the Nattoralinnguaq valley glacier (Fig. 10), and if so, this suggests that both ice bodies were still in place prior to 13.6 ka. The most westerly sample sites, Nag 16 and 17 respectively, show that the Itilleq ice stream persisted until as late as 10.3 ± 0.9 ka to 9.8 ± 0.9 ka (Table 2).

5.0 Discussion

5.1 LGM ice sheet thickness and extent

The CRN dates from the ridge to the north of the Nattoralinnguaq valley demonstrate that both the Itilleq and Nattoralinnguaq ice surfaces did not exceed 755 m asl during the build-up to the LGM and illustrate that a periglacial landscape above that has remained ice free for up to 140 ka, being last glaciated during MIS 6. The concordance between our ^{10}Be and ^{26}Al dates shows these areas were not covered by cold-based ice at any time during the last ca 140 ka, and hence, local trimlines represent upper ice surface LGM limits and not englacial thermal boundaries.

The extent and thickness of the Saalian glaciation in Greenland is poorly understood (Kelly *et al*., 1999; Adrielsson and Alexanderson, 2005.). However, our results provide a crude indication of ice surface elevation during MIS 6 being at least 1000 m asl in this area of West Greenland. Estimates of global eustatic sea-level drawdown during MIS 6 are ca -130 m (Waelbroeck *et al*., 2002), suggesting a global ice volume broadly similar to that during MIS 2. Our data from a single site should be treated with caution and require replication elsewhere, but nevertheless raise the possibility that the GIS may have made a larger contribution to global sea level fall during MIS 6 than during MIS 2.

As previously inferred by Kelly (1985), the occurrence of blockfield and tors above trimlines in central West Greenland provide a key geomorphic indicator that ice free conditions existed above the LGM ice sheet. The use of such geomorphic criteria in isolation has been questioned by Roberts *et al.* (2008) in southeast Greenland, where weathered terrain and blockfield was shown by CRN dating to be postglacial in age, but

the data presented here further reinforces the need to develop independent dating control on blockfield (and tor) terrain before their use as an indicator of ice thickness.

Maximum LGM ice sheet surface elevation is defined by Nag 5 (29.5 ±2.7 ka) and Nag 3 (55.4 ± 5.2 ka) to between 734 - 755 m asl. Following this, Nag 6 and 7 constrain ice sheet surface elevation to 574 - 498 m asl between 21.0 ± 0.7 ka and 20.3 ± 0.7 ka respectively (Table 2). This observation agrees broadly with the previous work of Kelly (1985) and the more recent field observations of Rinterknecht *et al.* (2009) who report CRN dates to the north of Sisimiut that limit LGM ice sheet surface extent to between 385- 720 m asl on the outer coast.

Taking these constraints and topography into account, ice sheet thickness along the Itilleq/Qingartaq coast in West Greenland approached ca 700 m and will have been ca 1000+ m in Itilleq fjord and Holsteinsborg dyb. This is in broad agreement to recent modelled ice sheet thicknesses for West Greenland. Using a three-dimensional thermo-mechanical model of GIS constrained by observations of relative sea-level (RSL) and geological field data of past ice extent, Simpson *et al.* (2009) model ice thickness over the Nattoralinnguaq and Sisimiut areas at ca 900 m asl (Fig. 11). These modelled ice sheet profile reconstructions suggest the LGM ice attained at least a mid-shelf position, probably forming the Outer Hellefisk moraines (Fig. 1), thus adding weight to a 'maximum' LGM ice sheet model for this part of the GIS. These projected outer shelf LGM limits also enable us to support the recent assertion that the Inner Hellefisk moraines may be of Younger Dryas age (Rinterknecht *et al.,* 2009; Simpson *et al*., 2009), but this remains conjectural until a robust chronology is available.

5.2 The timing and nature of deglaciation

Our CRN dates record a post LGM lowering of the ice sheet from 574 to 150 m asl surface between 21.0 ± 1.9 ka to 13.6 ± 1.42 ka along the interface between the Nattoralinnguaq valley glacier and the Itilleq ice stream. This relates to an overall surface downwasting rate of 0.06 m yr^{-1}, although higher rates (ca 0.12 m yr^{-1}) are possible after 15 ka in the middle of the valley. Sample Nag 10 demonstrates that the valley ice had a surface elevation less than 230 m asl by 16.3 ±1.5 ka (Tables 1 and 2), and by 13.6 ± 1.4 ka the ice surface had thinned further to ca 150 m asl within the lower valley (Tables 1 and 2; Fig. 5). With the local marine limit (ca 140 m asl) being reached at ca 11 kcal. yr BP (Fig. 12; Simpson *et al.*, 2009) the Nattoralinnguaq glacier will have become buoyant and calved quickly during this period, as indicated by the recessional De Geer moraines which mark successive grounding line retreat up to, and coincident with, marine limit formation.

The orientation of the De Geer moraines and the most westerly CRN ages infer that the Itilleq ice stream may have slightly lagged the Nattoralinnguaq valley glacier during retreat. The southwesterly arcuate track of the De Geer train shows it must have been constrained to the west by the ice stream. However, there is no geomorphological evidence to support ice stream calving or grounding line retreat as the ice stream moved eastward across the Qingartaq strandflat. This may be because the ice stream remained grounded due to thicker ice (Nag 16 limits the ice surface to 339 m asl at 9.8 ± 0.9 ka, Tables 1 and 2) and the buttressing effect of ice in Itilleq fjord which provided stability and extra ice flux until after 10 ka. Hence, in its final stages of deglaciation (ca 12 – 10 kcal. yr BP), the Nattoralinnguaq system was a small calving bay located on the southern edge of the larger Itilleq ice stream. Deglacial dates just to the north of Itilleq

based on marine shells confirm that the ice sheet had retreated to the present coast by 10.4 – 10.2 kcal. yr BP (Weidick, 1972; Kelly, 1973, 1979; Bennike and Björck, 2002).

5.3 Ice sheet response to climate forcing

Our new CRN dates show that the ice sheet surface started to thin after ca. 21.0 ± 1.9 ka, lowering from ca 570 m to 150 m by 13.6 ±1.42 ka at an average rate of 0.06 to 0.12 m yr^{-1}. The timing of this lowering coincides broadly with the period of rapidly increased air temperatures over Greenland recorded in the ice core records running up to the Bølling Interstadial (GIS1e) temperature maximum (Dahl-Jensen *et al*., 1998) (Fig. 13) and points to surface ablation as a key driver of early deglaciation. A similar mechanism has been invoked in southeast Greenland, where a rapid increase in air temperature after the Younger Dryas caused rapid ice downwasting and margin retreat (Roberts *et al*., 2008).

Relative sea-level rise is also likely to have influenced the timing and nature of deglaciation. During the initial post-LGM period, thick ice (particularly the ice streams situated in deep troughs, eg Holsteinsborg dyb ca 1000+ m of ice), would have been grounded and able to withstand initial rapid RSL rise. Simpson *et al.* (2009) predict that RSL in the study area rose rapidly from 16 kcal. yr BP to reach a highstand of ca 100 m asl at 11 kcal. yr BP (Fig. 12). By this time, we suggest that the high RSL would have destabilised relatively thin ice (ca <400 m thick) grounded on shallower shelf areas (ca 300 m water depth). In contrast, it was only by ca 10 kcal. Yr BP that Holsteinsborg ice stream was sufficiently thin (ca < 600 m of ice) to become destabilized by RSL rise, once water depths of ca 500 m were attained.

The influence of increased ocean temperatures must also have affected ice retreat from the shelf. The earliest dates for the arrival in West Greenland of the warm West Greenland Current (WGC) are 9.7 – 10.6 kcal. yr BP based on molluscs from Thule area (Feyling-Hanssen and Funder, 1990), whilst diatom data suggests conditions as warm as present in the North Water Polynya (Northern Baffin Bay) by 9.8 kcal. yr BP (Levac *et al.,* 2001). Along the southwest coast of Greenland this evidence is somewhat fragmentary, but Lloyd *et al.* (2005) report a weak WGC signal in southern Disko Bugt by 9.2 ka cal. BP. Funder and Weidick (1991) suggest that ocean temperatures were 1 - 3° C warmer than present at this time and this would have accelerated ice sheet retreat through enhanced marginal or basal thinning, as recently observed at Jakobshavn Isbræ (Holland *et al*., 2008)

The Nattoralinnguaq glacier was likely more sensitive to climate forcing. With its small catchment area (partially blind 15 km to the east) and valley floor being predominantly above the local marine limit to the east, the glacier was vulnerable to rapid thinning by surface melt. Taking topography into account, by 16.3 ± 1.5 ka (Nag 10; Tables 1 and 2; Fig. 5) ice thickness was already less than ca 130 m, and potentially less than less than 50 m by 13.6 ± 1.4 ka (Nag 15; Tables 1 and 2; Fig. 5). With rapid thinning, the western end of the glacier would have become buoyant soon after 16.3 ± 1.5 ka and likely calved back to a mid valley position by ca 11 ka cal. BP, the modelled age of the marine limit (Simpson *et al.,* 2009, Fig. 12). The De Geer moraine train therefore corresponds to full glacial sea conditions at this time.

5.4 Ice streams and climate forcing

Our results demonstrate that the ice streams and adjacent ice sheets probably experienced different styles and chronologies of deglaciation in West Greenland. Variations in ice thickness and source area, as well as elevation with respect to sea bed topography and prevailing RSL were each significant in controlling spatial and temporal variations. Our ice thickness data, coupled with the CRN chronology, suggest that initial ice retreat from the shelf was likely a result of surface ablation and not RSL rise. However, by ca 11 ka cal. BP, as RSL rose to its maximum, so thinner areas of ice on the shelf would have also become vulnerable to buoyant lift-off and retreat by calving. Small valley systems with only local, non-ice sheet source areas, such as the Nattoralinnguaq valley glacier, would have been more susceptible to RSL rise compared with the thicker ice in the Holsteinsborg and Itilleq ice streams, which were fed by the ice sheet via deep fjords. Ice thickness in these troughs significantly reduced calving instabilities during early deglaciation, but increasing coastal water depths between 12.5 - 11 kcal. yr BP eventually triggered ice stream retreat from the inner shelf (Fig. 12).

Our new chronology differs from that previously proposed for West Greenland. Funder and Hansen (1996) suggest a two stage deglaciation, with early retreat from shelf areas between ca 15 and 10 kcal. yr BP, followed by retreat of the terrestrial portion of the ice sheet after ca 10 kcal. yr BP. However, the correspondence between our CRN ages and radiocarbon dates along the coast indicate that ice did not leave the shelf early, but remained grounded on the inner shelf until at least 10 ka BP, well into the start of the Holocene (recently defined as 11.7k cal yr b2 k (before AD 2000); Walker *et al.,* 2009). The key control on both ice sheet and ice stream retreat after the Younger Dryas appears to have been a combination of a high RSL (although this fell quickly from the marine limit due to glacio-isostatic rebound), a rapid increase in air temperatures, as well as the establishment of the warm West Greenland Current that combined to drive the ice inland from the present coast.

In the wider context of West Greenland, our new findings from the Itilleq area are in close agreement with the chronology for ice margin retreat from Disko Bugt. In the latter, RSL records and offshore sediment cores suggest that Jakobshavn Isbræ also remained on the outer shelf until ca 10 kcal. yr BP before retreating rapidly to the east of the bay (Long and Roberts, 2003; Lloyd *et al*., 2005). Long and Roberts (2002) note that the ice stream here was also able to withstand the effects of Late Glacial RSL change, including the rapid rise associated with meltwater Pulse 1a, and suggest that ice thickness and high rates of ice discharge promoted ice stream stability.

On the east and southeast Greenland shelf, troughs such those at Kangerlussuaq and Gyldenløves fjord have also been hypothesised to have acted as ice stream pathways throughout the Quaternary (Solheim *et al.,* 1998; Lykke-Andersen, 1998). Roberts *et al*. (2008) speculated on three regional mechanisms that controlled ice margin behaviour during overall deglaciation in southeast Greenland. Offshore data from Kangerlussuaq Trough and to the south of Sermilik Fjord constrain deglaciation of the outer shelf to 15.7 – 14.6 kcal. yr BP(Jennings *et al.,* 2002, 2006; Kuijpers *et al.,* 2003). This may have been partially driven by rising global sea-level and increasing air temperatures, but Jennings *et al.* (2006) infer rapid basal ablation of the shelf based ice sheet and ice streams by influx of the warm Irminger current during the Allerød (13.4 – 12.8 kcal. yr BPand the Younger Dryas (12.8 - 12.0 kcal. yr BP). Both the ice sheet and large ice streams such as Helheim glacier had retreated to the present east coast by 11 kcal. yr BP, with warm post Younger Dryas air temperatures driving rapid ice downwasting at

low altitudes, and calving in deep water troughs triggering marginal retreat to coastal pinning points.

6.0 Conclusions

Regional ice flow patterns to the south of Sisimiut, West Greenland show that the LGM ice sheet expanded southwest on to the shelf, strongly influenced by a topographically constrained ice stream flowing into Holsteinsborg dyb. Striae and roche moutonnée long axes orientations along the coast to the south of Itilleq fjord, show the Itilleq fjord ice cross-cutting the coast in a southwesterly direction and deflecting local valley glaciers during the build-up to and decay from the LGM.

The LGM surface elevation of the ice sheet is constrained by periglacial geomorphology consisting of blockfield and tors above local trimlines, and by CRN ages that demonstrate nunatak surfaces dating to 101 – 142 ka which have remained unglaciated since MIS 6. The extent and thickness of MIS 6 ice remains poorly constrained, but these CRN dates suggest ice surface was at least 1000 m asl in this area and that the maximum ice sheet volume in Greenland during MIS 6 was greater than that in MIS 2. The CRN data also confirm that trimlines and high blockfield terrain in West Greenland can provide geomorphic constraints on the elevation of the LGM ice surface, and that use of ^{10}Be and ^{26}Al analysis in combination can determine whether cold-based ice or englacial thermal boundaries played a role in trimline and blockfield development.

The maximum surface elevation of the LGM ice sheet was between 750 – 810 m asl, which coupled with shelf moraine morphology adjacent to Holsteinsborg dyb, shows ice extended westwards to at least a mid-shelf position, and probably the outer shelf edge and the Outer Hellefisk moraines. The timing of early shelf deglaciation is unknown, but the early downwasting of the Nattoralinnguaq and Itilleq glaciers coincides with the period of increased air temperatures over Greenland running up to the Bølling Interstadial (GIS1e) at ca 14 kcal. yr BP. Sea-level forcing under full glacial sea conditions between 12-11 kcal. yr BP helped drive the ice sheet off the inner shelf, but ice streams may have remained more stable during this period due to increased ice thickness and ice discharge. However, by ca 10 kcal. yr BP, further increases in air temperature combined with the influx of the warm West Greenland Current caused ice retreat inland of the present coastline.

Acknowledgements

This work was supported by the University of Durham and NERC CIAF Grant No: 9035-0407. We would like to thank Will Todd, Leanne Wake and Sarah Woodroffe for their help in the field. Allan Davidson for mineral separation and assistance with chemical sample preparation, Leticia Miguéns-Rodríguez and Valérie Olive for Al determination with ICP-MS. The Design and Imaging Unit, Department of Geography, Durham University are thanked for the production of figures. We thank Svend Funder and an anonymous reviewer for useful and constructive comments.

References

Adrielsson, L., Alexanderson, H., 2005. Interactions between the Greenland Ice Sheet and the Liverpool Land coastal ice cap during the last two glaciation cycles. Journal of Quaternary Science 20, 269-283.

Balco, G., Stone, J.O., Lifton, N.A., Dunai, T.J., 2008. A complete and easily accessible means of calculating surface exposure ages or erosion rates from ^{10}Be and ^{26}Al measurements. Quaternary Geochronology 3, 174-195.

Ballantyne, C.K., 1997. Periglacial trimlines in the Scottish Highlands. Quaternary International 38/39, 119 - 136.

Ballantyne, C.K., Schnabel, C., Xu, S., 2009. Exposure dating and reinterpretation of coarse debris accumulations (rock glaciers) in the Cairngorm Mountains, Scotland. Journal of Quaternary Science 24, 19-31.

Bennike, O., Björck, S., 2002. Chronology of the last recession of the Greenland Ice Sheet. Journal of Quaternary Science 17, 211-219.

Bennike, O., Björck, S., Lambeck, K., 2002. Estimates of South Greenland late-glacial ice limits from a new relative sea level curve. Earth and Planetary Science Letters 197, 171-186.

Bierman, P.R., Marsella, K.A., Patterson, C., Davis, P.T., Caffee, M., 1999. Mid-Pleistocene cosmogenic minimum-age limits for pre-Wisconsin glacial surfaces in southwestern Minnesota and southern Baffin Island: a multiple nuclide approach. Geomorphology 27, 25–39.

Box, J.E, Bromwich, D.E., Veenhuis, B.A., Bai, L.-S., Stroeve, J.E., Roger, J.C., Steffen, K., Haran,T., Wang, H.H., 2006. Greenland Ice Sheet surface mass balance variability (1988–2004) from Calibrated Polar MM5 Output. Journal of Climate 19, 2783 – 2800

Brett, C.P., Zarudzki, E.F.K., 1979. Project Westmar, a shallow marine geophysical survey on West Greenland continental shelf. Rapport 87, Grønlands Geologiske Undersøgelse, Copenhagen.

Chen, J.L., Wilson, C.R., Tapley, B.D., 2006. Satellite gravity measurements confirm accelerated melting of Greenland Ice Sheet. Science 313, 1958-1960.

Dahl-Jensen, D., Mosegaard, K., Gundestrup, N., Clow, G.D., Johnsen,S.J., Hansen, A.W., Balling, N., 1998. Past temperatures directly from the Greenland ice sheet. Science 282, 268–271.

Donner, J., Jungner, H., 1975. Radiocarbon dating of shells from marine deposits in the Disko Bugt area, West Greenland. Boreas 4, 25–45.

Dunne, J., Elmore, D., Muzikar, P., 1999. Scaling factors for the rate of production of cosmogenic nuclides for geometric shielding and attenuation at depth on sloped surfaces. Geomorphology 27, 3-11.

Feyling-Hanssen, R.W., Funder, S., 1990. Flora and fauna. In: Funder, S. (Ed.), Late Quaternary Stratigraphy and Glaciology in the Thule Area, Vol. 22. Geoscience, Meddelelser om Gronland,pp. 19–33.

Funder, S., 1989. Quaternary geology of the ice-free areas and adjacent shelves of Greenland. In: Fulton, R.J. (Ed.), Quaternary Geology of Canada and Greenland. Geological Survey of Canada and Greenland, pp. 743–792.

Funder, S., Hansen, L., 1996. The Greenland ice sheet - a model for its culmination and decay during the after the Last Glacial Maximum. Bulletin of the Geological Society of Denmark 42, 137–152.

Funder, S., Weidick, A., 1991. Holocene boreal molluscs in Greenland - palaeoceanographic implications. Palaeogeography, Palaeoclimatology, Palaeoecology 85, 123–135.

Glasser, N., Warren, C., 1990. Medium scale landforms of glacial erosion in southern Greenland: process and form. Geografiska Annaler 72, 211–215.

Gordon, J. E., 1981: Ice scoured topography and its relationships to bedrock structure and ice movement in parts of northern Scotland and West Greenland. Geografiska Annaler 63, 55–65.

Gosse, J.C., Phillips, F.M., 2001. Terrestrial in situ cosmogenic nuclides: theory and applications. Quaternary Science Reviews 40, 1475-1560.

Håkansson, L., Briner, J., Alexandersson, H., Aldahand, A., Possnerte, G., 2007. ^{10}Be ages from central East Greenland constrain the extent of the Greenland ice sheet during the Last Glacial Maximum. Quaternary Science Reviews 26, 2316–2321.

Håkansson, L., Hjort, C., Möller, P., Briner, J., Aldahan, A., Possnert, G., 2008. Late Pleistocene glacial history of Jameson Land, central East Greenland, derived from cosmogenic ^{10}Be and ^{26}Al exposure dating. Boreas 38, 244-260,

Heyman, J., Hättestrand, C., 2006. Morphology, distribution and formation of relict marginal moraines in the Swedish Mountains. Geografiska Annaler, 88A, 253–265. 558.

Holland, D.M., Thomas, R.H., deYoung,B., Ribergaard, M.H., Lyberth, B., 2008. Acceleration of Jakobshavn Isbrae triggered by warm sub-surface ocean waters. Nature Geoscience, doi:10.1038.

Howat, I.M., Joughin, I., Tulaczyk, S., Gogineni, S., 2005. Rapid retreat and acceleration of Helheim Glacier, East Greenland. Geophysical Research Letters 32, L22502, doi:10.1029/2005GL024737.

Ingólfsson, O., Frich, P., Funder, S. & Humlum, O., 1990. Palaeoclimatic implications of an early Holocene glacier advance on Disko Island, West Greenland. Boreas 19, 297-311.

Jennings, A.E., Gronvold, K., Hilberman, R., Smith, M., Hald, M., 2002. High-resolution study of Icelandic tephras in the KangerlussuqTrough, Southeast Greenland, during the last deglaciation. Journal of Quaternary Science 7, 747–757.

Jennings, A. E., Hald, M., Smith, M., 2006. Freshwater forcing from the Greenland Ice Sheet during the Younger Dryas: evidence from southeastern Greenland shelf cores. Quaternary Science Reviews 25, 282-298.

Joughin, I., 2006. Climate change - Greenland rumbles louder as glaciers accelerate. Science 311, 1719-1720.

Kelly, M., 1973. Radiocarbon dated shell samples from Nordre Strømfjord, West Greenland. Rapport 59, Grønlands Geologiske Undersøgelse, Copenhagen.

Kelly, M., 1979. Comments on the implications of new radiocarbon dates from the Holsteinsborg region, central West Greenland. Rapport 95, Grønlands Geologiske Undersøgelse, Copenhagen;

Kelly, M.,1985. A review of the Quaternary geology of western Greenland. In: Andrews, J.T. (Ed.), Quaternary Environments in Eastern Canadian Arctic, Baffin Bay and Western Greenland. Allen and Unwin, Boston, pp. 461-501.

Kelly, M., Funder, S., Houmark-Nielsen, M., 1999. Quaternary glacial and marine environmental history of northwest Greenland: a review and re-appraisal. Quaternary Science Reviews 18, 373 – 392.

Kelly, M.A., Lowell, T.A., Hall, B.L., Schaefer, J.M., Finkel, R.C., Goehring, B.M., Alley, R.B., Denton, G.H., 2008. A ^{10}Be chronology of Lateglacial and Holocene mountain glaciation in the Scoresby Sund region, east Greenland: implications for seasonality during lateglacial time. Quaternary Science Reviews 27, 2273-2282.

Krabill, W., Hanna, E., Huybrechts, P., Abdalati, W., Cappelen, J., Csatho, B., Frederick, E., Manizade, S., Martin, C., Sonntag, J., Swift, R., Thomas, R.,Yungel, J., 2004. Greenland ice sheet: increased coastal thinning. Geophysical Research Letters 31, L24402, 10.1029/2004GL020444.

Kuijpers, A., Troelstra, S.R., Prins, A., Linthout, K., Akhmetzhaov, A., Bouryak, S., Bachmann, M.F. Lassen, S., Rasmussen, S., Jensen, J.B., 2003. Late Quaternary sedimentary processes and ocean circulation changes at the southeast Greenland margin. Marine Geology 195, 109-129.

Levac, E., De Vernal, A., Blake, W., 2001. Sea-surface conditions in northernmost Baffin Bay during the Holocene: Palynological evidence. Journal of Quaternary Science 16, 353–363

Lindén, M., Möller, P., 2005. Marginal formation of De Geer moraines and their implications to the dynamics of grounding-line recession. Journal of Quaternary Science 20, 113–133.

Lloyd, J.M., Park L.A., Kuijpers, A., Moros, M., 2005. Early Holocene palaeoceanography and deglacial chronology of Disko Bugt, West Greenland. Quaternary Science Reviews 24, 1741–1755.

Lloyd, J.M., 2006. Late Holocene environmental change in Disko Bugt, West Greenland: interaction between climate, ocean circulation and Jakobshavn Isbrae. Boreas 35, 35-49.

Long, A.J., Roberts, D.H., Wright, M.R., 1999. Isolation basin stratigraphy and Holocene relative sea-level change on Arveprinsen Eijland, Disko Bugt, West Greenland. Journal of Quaternary Science 14, 323–345.

Long, A.J., Roberts, D.H., 2002. A revised chronology for the Fjord Stade moraine in Disko Bugt, West Greenland. Journal of Quaternary Science 17, 561–579.

Long, A.J., Roberts, D.H., 2003. Late Weichselian deglacial history of Disko Bugt, West Greenland, and the dynamics of Jakobshavn Isbræ ice stream. Boreas 32, 208 -226.

Long, A.J., Roberts, D.H., Rasch, M.R., 2003. New observations on the relative sea-level and deglacial history of Greenland from Innaarsuit, Disko Bugt, Quaternary Research 60, 162-171.

Long, A.J., Roberts D.H., Dawson, S., 2006. Early Holocene history of the West Greenland Ice Sheet and the GH-8.2 ka cal. yr BP event. Quaternary Science Reviews 25, 904-922.

Long, A.J., Roberts, D.H., Simpson, M., Dawson, S., Milne, G., Huybrechts, P., 2008. Late Devensian relative sea-level changes and ice sheet history of southeast Greenland. Earth and Planetary Science Letters 272, 8-18.

Long, A.J., Woodroffe, S. A., Dawson, S., Roberts, D.H., Bryant, C.L., 2009. Late Holocene relative sea-level rise and the Neoglacial history of the Greenland Ice Sheet. Journal of Quaternary Science, ISSN 0267-8179.

Lykke-Andersen, H., 1998. Neogene–quaternary depositional history of the East Greenland shelf in the vicinity of leg 152 shelf sites. In: Saunders, A.D., Larsen, H.C., and Wise, S.W., Jr. (Eds.), Proceedings of the Ocean Drilling Program, Scientific Results,152, pp. 29-38.

Marsella, K.A., Bierman, P.R., Tompson Davis, P., Caffee, M.W., 2000. Cosmogenic ^{10}Be and ^{26}Al ages for the Last Glacial Maximum, eastern Baffin Island, Arctic Canada. GSA Bulletin 112, 1296-1312.

McConnell, J.R., Arthern, R.J., Mosely-Thompson, E., Davis, C.H., Bales, R.C., Thomas, R., Burkhart, J.F., Kyne, J.D., 2000. Changes in Greenland ice sheet elevation attributed primarily to snow accumulation variability. Nature 406, 877-879.

Nishiizumi, K., Imamura, M.,Caffee, M.W., Southon, J.R.Finkel, R.C., McAninch, J., 2007. Absolute calibration of ^{10}Be AMS standards. Nuclear Instruments and Methods in Physics Research B, 258, 403–413.

Powell, R., 1990. Glaciomarine processes at grounding-line fans and their growth to ice contact deltas. In: Dowdeswell, J.A. and Scourse, J.D. (Eds.), Glaciomarine environments: processes and sediments. Geological Society special Publication 53, pp. 53 – 73.

Rignot, E., Kanagaratnam, P., 2006. Changes in the velocity structure of the Greenland Ice Sheet. Science 311, 986-990.

Rinterknecht, V.R., Gorokhovich, Y., Schaefer, J.M., Caffee, M. 2009. Preliminary ^{10}Be chronology for the last deglaciation of the western margin of the Greenland Ice Sheet. Journal of Quaternary Science 24, 270–278

Roberts, D.H., Long, A.J., 2005. Streamlined bedrock terrain and fast ice flow, Jakobshavn Isbræ, West Greenland: implications for ice stream and ice sheet dynamics. Boreas 34, 25-42.

Roberts, D.H., Long, A.J., Schnabel, C., Simpson, M., Freeman, S., 2008. The deglacial history of the southeast sector of the Greenland ice sheet during the Last Glacial Maximum. Quaternary Science Reviews 27, 1505-1516.

Simpson, M.R., Milne, G., Huybrechts, P., Long, A.J., 2009. Calibrating a glaciological model of the Greenland ice sheet from the last glacial maximum to present-day using field observations of relative sea level and ice extent. Quaternary Science Reviews, doi:10.1016/j.quascirev.2009.03.004.

Solheim, A., Faleide, J.I., Andersen, E.S., Elverhoi, A., Forsberg, C.F., Vanneste, K., Uenzelmann-Neben, G., Channell, J.E.T., 1998. Late Cenozoic seismic stratigraphy and glacial geological development of the East Greenland and Svalbard-Barents Sea continental margins. Quaternary Science Reviews 17, 155–184.

Sommerhoff, G., 1975. Glaziale Gestaltung und marine Überformung der Schelfbänke vor SW-Grönland. Polarforschung 45, 22–31.

Sparrenbom, C., Bennike, O., Björck, S., Lambeck, K., 2006. Relative sea-level changes since 15,000 cal. yrs BP in the Nanortalik area, southern Greenland. Journal of Quaternary Science 21, 29-48.

Sugden, D. E., Glasser, N., Clapperton, C.M., 1992. Evolution of large roche moutonnées. Geografiska Annaler 74, 253–264.

Tarasov, L., Peltier, W.R., 2002. Greenland glacial history and local geodynamic consequences. Geophysical Journal International 150, 190-229.

Ten Brink, N.W., Weidick, A., 1975. Holocene history of the Greenland ice sheet based on radiocarbon-dated moraines in West Greenland. Grønlands Geologiske Undersøgelse Bulletin, 113, 1-44.

van Tatenhove, F.G., Fabre, A., Greve, R., Huybrechts, P., 1996. Modelled ice-sheet margins of three Greenland ice-sheet models compared with a geological record from ice-marginal deposits in central West Greenland. Annals of Glaciology 23, 52–58.

Velicogna, I., Wahr, J., 2006. Acceleration of Greenland ice mass loss in spring 2004. Nature 443, 329-331.

Waelbroeck, C., Labeyrie, L., Michel, E., Duplessy, J.C., McManus, J.F., Lambeck, K., Balbon, E., Labracherie, M., 2002. Sea-level and deep water temperature changes derived from benthic foraminifera isotopic records. Quaternary Science Reviews, 21 295–305

Walker, M., Johnsen, S., Rasmussen, S. O., Popp, T., Steffensen, J.-P., Gibbard, P., Hoek, W., Lowe, J., Andrews, J., Bjo¨ rck, S., Cwynar, L. C., Hughen, K., Kershaw, P., Kromer, B., Litt, T., Lowe, D. J., Nakagawa, T., Newnham, R., Schwander, J., 2009. Formal definition and dating of the GSSP (Global Stratotype Section and Point) for the base of the Holocene using the Greenland NGRIP ice core, and selected auxiliary records. Journal of Quaternary Science, 24, 3–17.

Weidick A., 1972. Holocene shore-lines and glacial stages in Greenland: an attempt at correlation. Rapport 41, Grønlands Geologiske Undersøgelse, Copenhagen.

Weidick, A., 1996. Neoglacial changes of ice cover and sea level in Greenland - a classical enigma. In: Grønnow, B. (Ed). The palaeo-Eskimo cultures of Greenland: new perspectives in Greenlandic archaeology,. Danish Polar Center, University of Copenhagen, pp. 257-270.

Weidick, A., Kelly, M., Bennike, O., 2004. Late Quaternary development of the southern sector of the Greenland Ice Sheet, with particular reference to the Qassimuit lobe. Boreas 33, 284-299.

Weidick, A., Bennike, O., 2007.Quaternary glaciation history and glaciology of Jakobshavn Isbræ and the Disko Bugt region, West Greenland: a review. Geological Survey of Denmark and Greenland Bulletin, No 14.

Wilson, P., Bentley, M.J., Schnabel, C., Clark, R., Xu, S., 2008. Stone run (block stream) formation in the Falkland Islands over several cold stages, deduced from cosmogenic isotope (^{10}Be and ^{26}Al) surface exposure dating. Journal of Quaternary Science 23, 461-473.

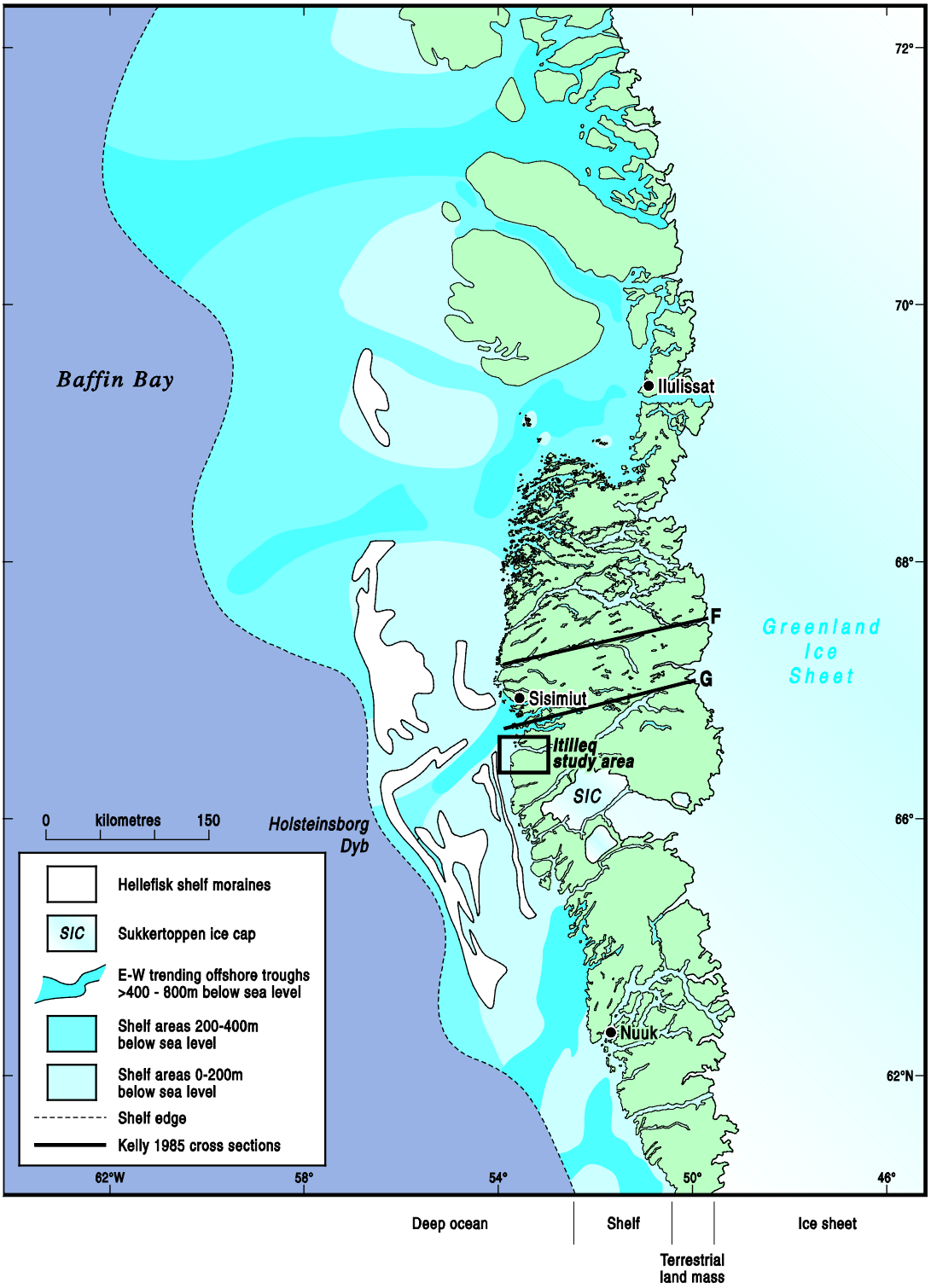

Fig. 1. The west coast of Greenland. Note the position of the present ice sheet margin and fjord systems trending east to west. The shelf area is cross-cut by several deep troughs which routed ice streams offshore during successive glacial periods. Note also the position of the Inner and Outer Hellefisk moraine complexes (Brett and Zarudski, 1979) and two topographic profiles reconstructed by Kelly (1985).

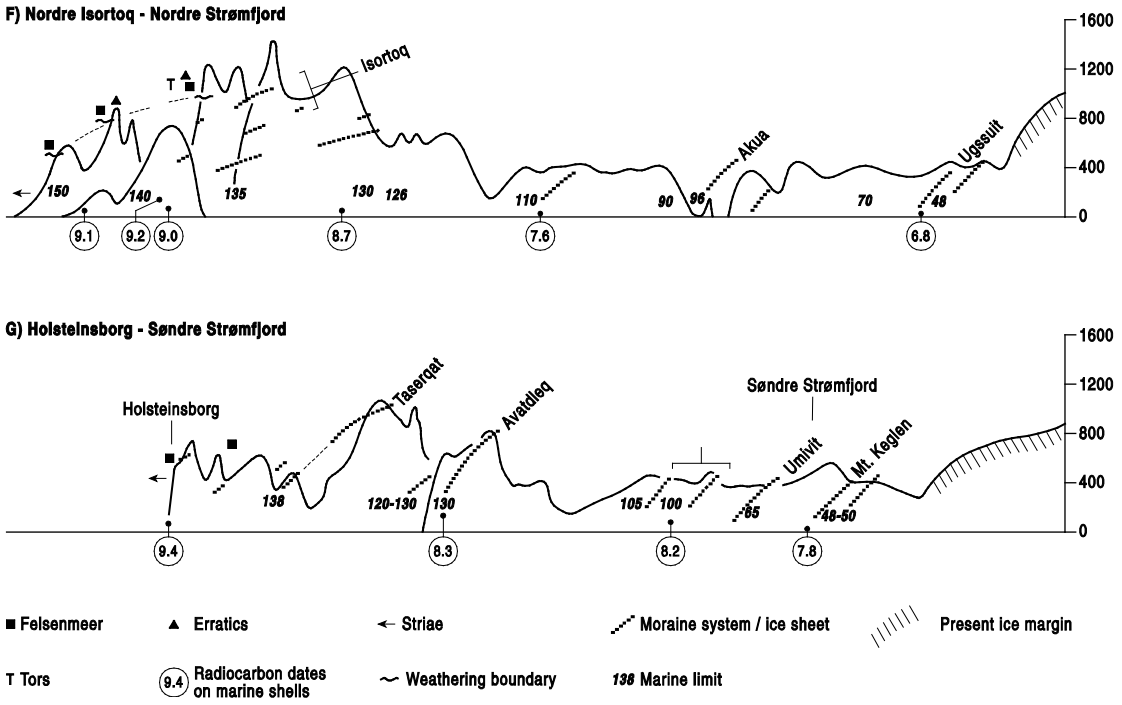

Fig. 2. Two topographic cross sections reconstructed by Kelly (1985). These show the previous ice sheet marginal positions (moraines), striae, erratics, trimlines, blockfield, tors and deglacial dates in the region to the north of the current study site.

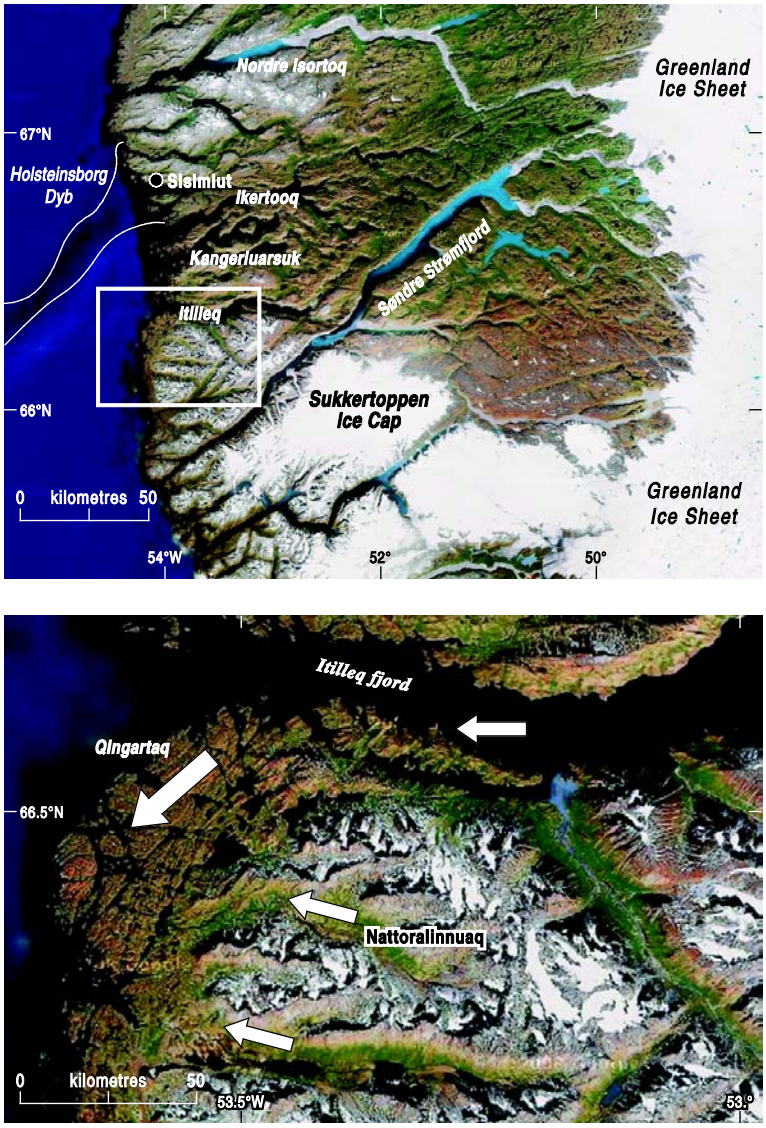

Fig. 3. An overview of the Itilleq field region. Fig. 3a shows the regional topography with deep fjords running east to west and northeast to southwest as controlled by the regional geology. Ikertooq and Kangerluarsuk fjords would have routed ice offshore into Holsteinsborg dyb, while ice flowing down Søndre Strømfjord and into Itilleq fjord would have flowed southwestwards to the south of Holsteinsborg dyb. Fig. 3b shows the study area, with east/west trending local valleys emerging from the mountainous terrain to the west of Sukkertoppen ice cap on to a low elevation, undulating coastal plain composed of heavily glacially abraded bedrock (arrows denote approximate ice flow direction).

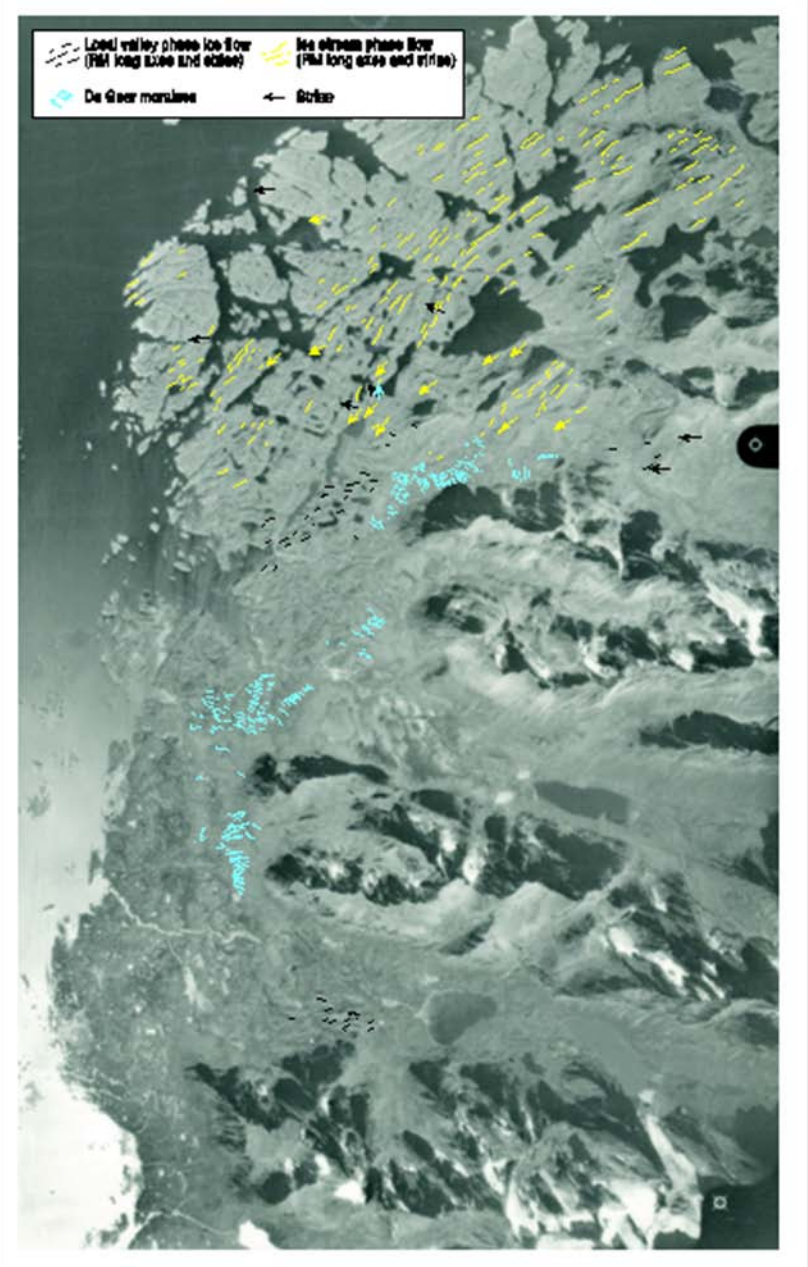

Fig. 4. Aerial photograph of the Itilleq coastal area showing roche moutonnée long axes, striae and De Geer moraine patterns. Note the dominant roche moutonnée long axes running northeast to southwest. This is locally influenced by bedrock structure, but ice flow directions have been verified using striae orientations.

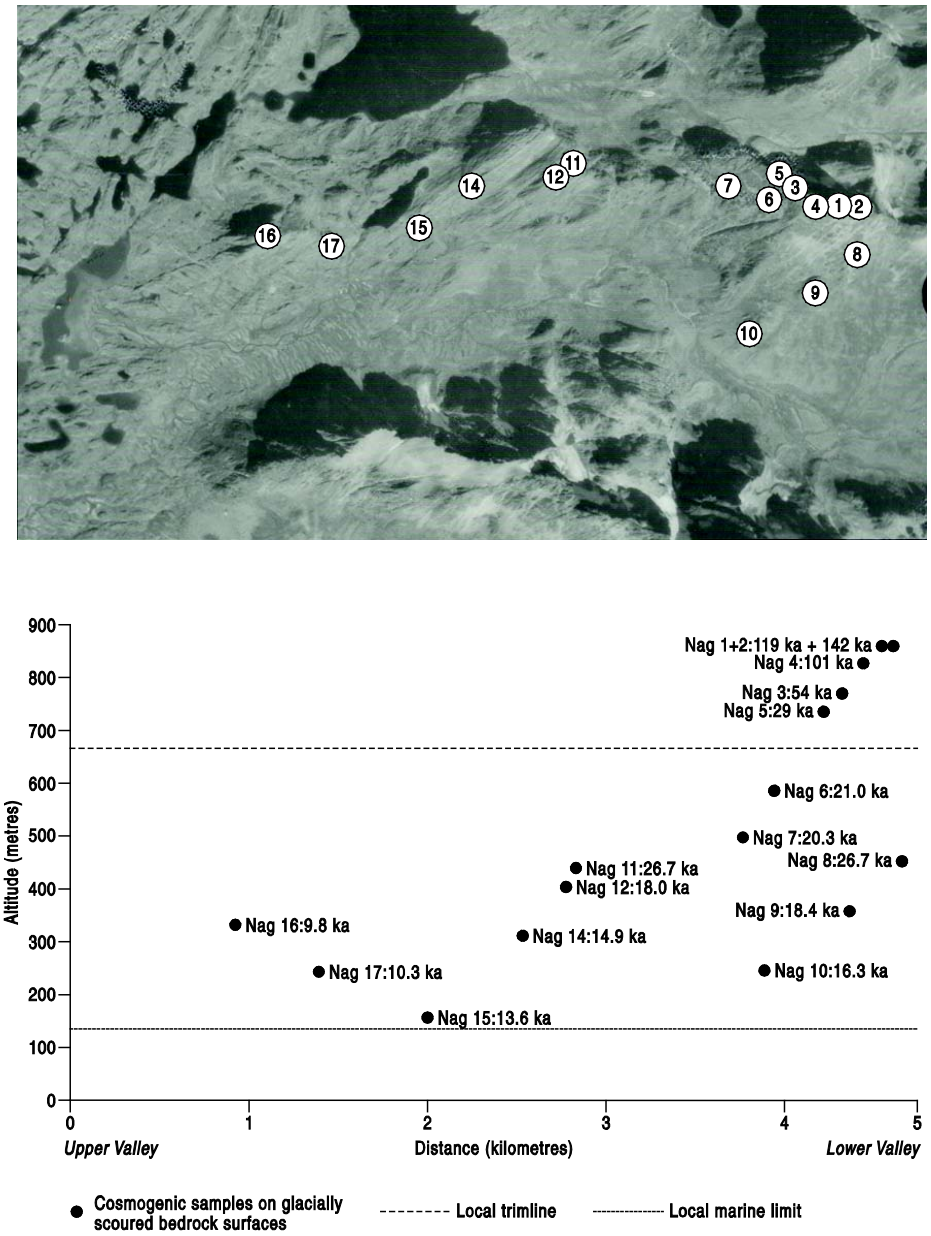

Fig. 5. The location, age and elevation of cosmogenic surface exposure samples taken from within the Nattoralinnguaq valley and adjacent ridge areas.

Fig. 6. View looking eastward up the Nattoralinnguaq valley showing mountainous terrain up to 1200 m asl. Summits and ridges are characterised by blockfield and tor development and often separated by local trimlines from glacially abraded terrain below (dotted line marks this transition).

Fig. 7. Blockfield terrain above 800 m asl on the ridge to the north of the Nattoralinnguaq valley. Note the angularity of the blocks which lack any definitive signs of glacial erosion.

Fig. 8. Glacially eroded terrain with roche moutonnée below 500 m asl in the upper Nattoralinnguaq valley.

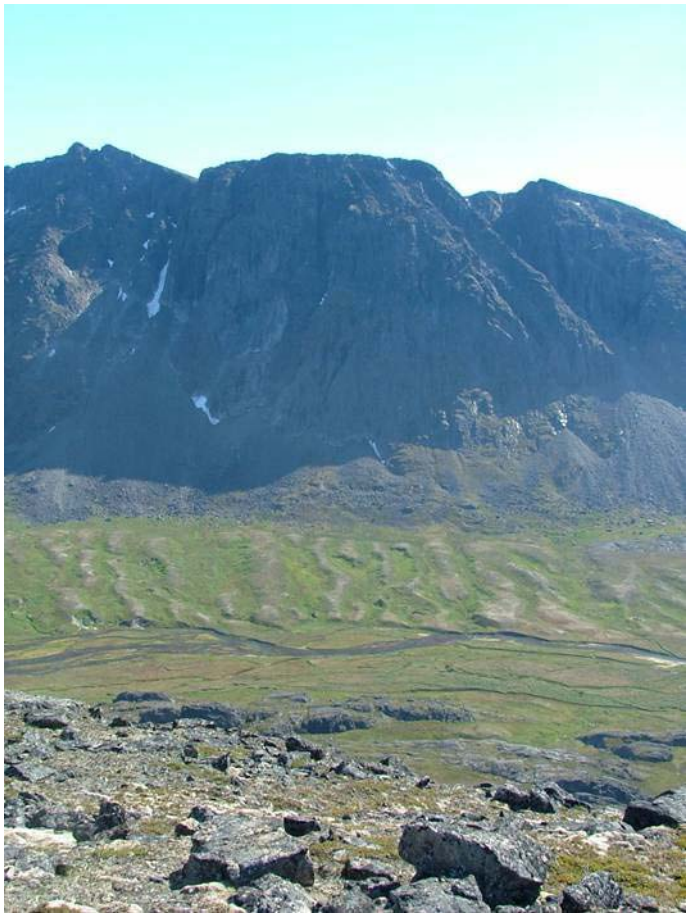

Fig. 9. De Geer recessional moraines on the floor of the Nattoralinnguaq valley below the local marine (ca 140 m asl). Note their uniform spacing and height, and slope conformity, potentially controlled by transverse crevasse spacing, each ridge representing a small subaqueous push moraine composed of ice proximal rainout sediments.

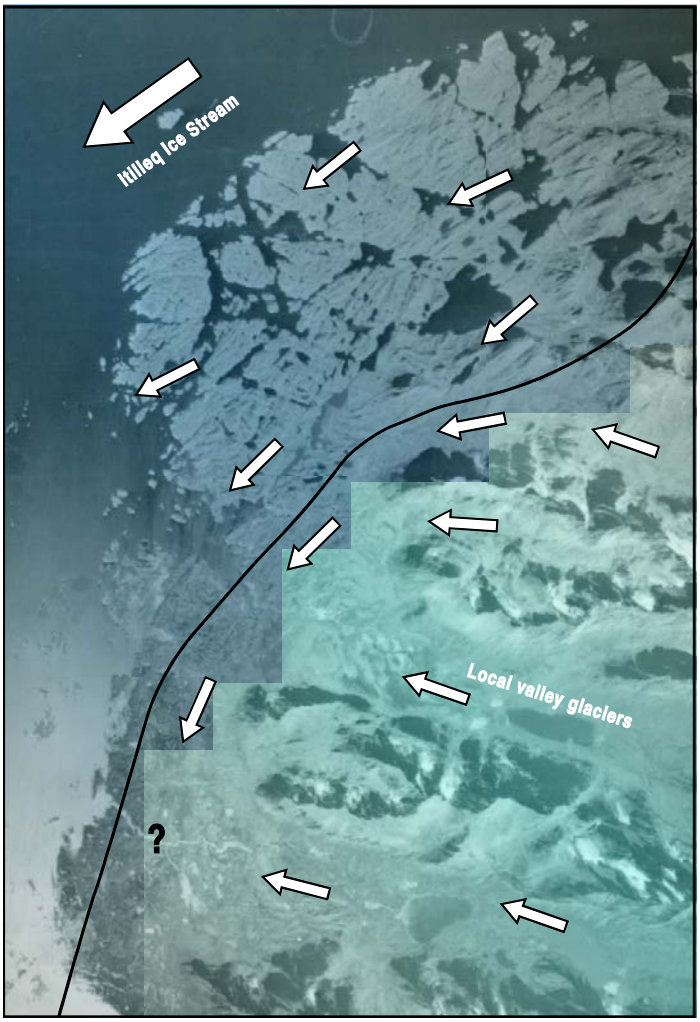

Fig.10. Simplified reconstruction of ice flow pathways across the Itilleq coast. Note deflection of local valley glaciers (eg.) by the Itilleq ice stream flowing southwestwards across the outer coast, and the distinctive arcuate recessional path of the De Geer moraine train beyond the Nattoralinnguaq valley, demonstrating that the Itilleq ice stream remained in place as the Nattoralinnguaq glacier calved headward.

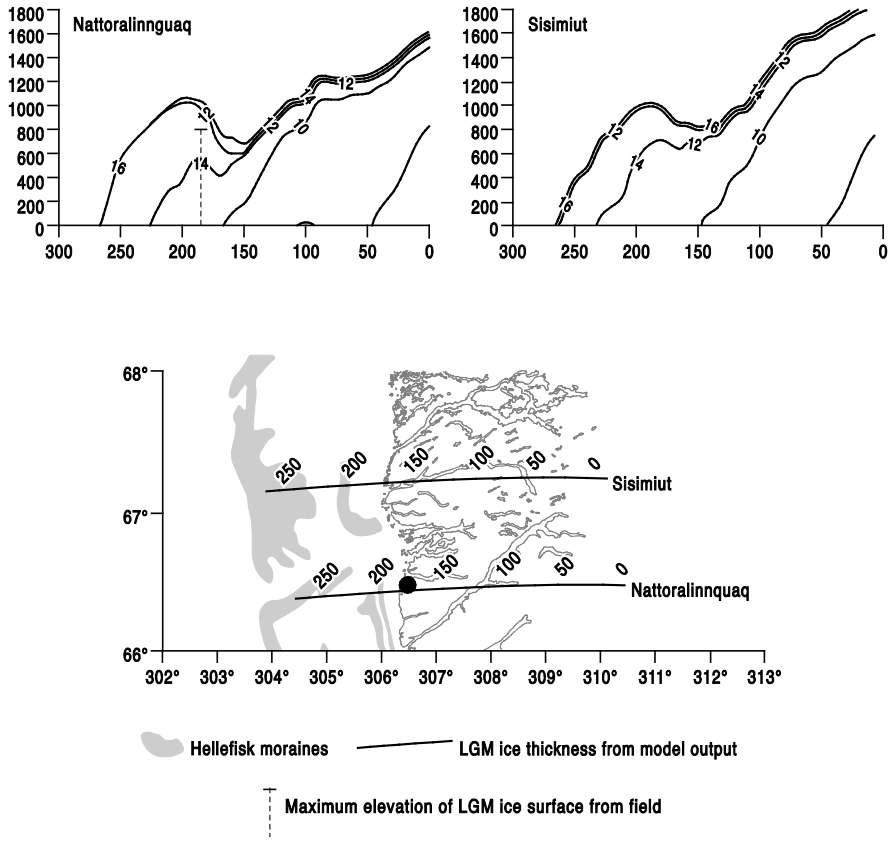

Fig 11. Reconstructed ice sheet surface elevations for 16, 14, 12 and 10 ka BP from Simpson *et al*. (2009). Note the maximum surface elevation of the ice sheet over the field area is 800 -1000m asl, crudely matching our field observations which place the ice surface to a maximum of 755 -813 m asl during the LGM. The model also predicts significant ice thinning by 14 ka BP, but re-expansion of the ice sheet at 12 ka BP due to Younger Dryas cooling. Predicted deglaciation by 10 ka contradicts our cosmogenic ages which suggest the Itilleq ice stream remained on the coast until 9.9 ka.

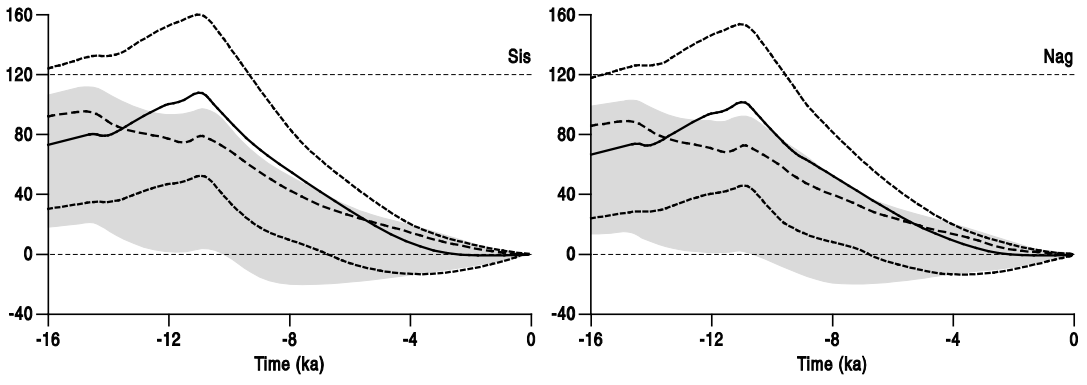

Fig. 12. Relative sea-level curves reconstructed for the Sisimuit and Nattoralinnguaq areas (Simpson *et al.*, 2009). The blacklines represent the optimal Huy 2 sea-level predictions using a mid-shelf mask to constrain ice sheet maximum expansion during the LGM. Note sea-level rise prior to ca 11 ka BP driven global eustatic sea-level rise, sea-level fall post ca 11 ka BP due to crustal unloading, and marine limit depicted at ca 120 m asl.

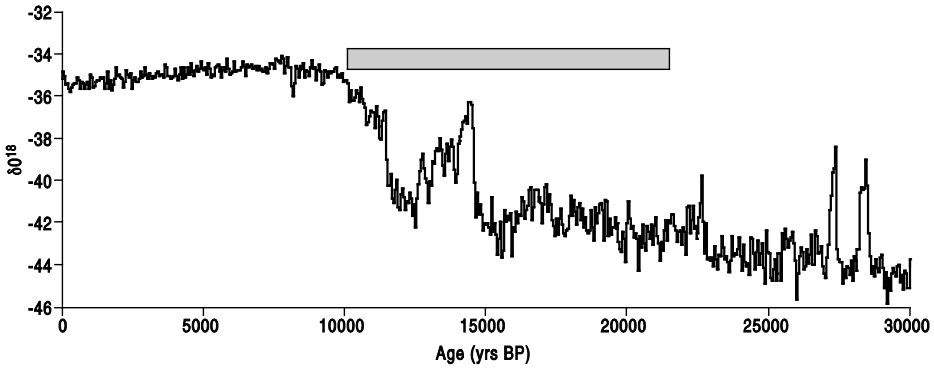

Fig. 13. The NGRIP temperature record for the last 30 ka. Note the overall increase in air temperatures between 21-14ka BP which overlap with our exposure ages (21.0 ka/Nag 6 to 13.6 ka/Nag 15 – grey bar). This period of warming would have driven significant surface ablation across the Itilleq region, prior to the marine destabilisation of the Nattoralinnguaq glacier.

Table 1. Details of the samples collected from the Nattoralinnguaq valley giving sample position, altitude, topographic shielding and thickness attenuation.

Sample code	Latitude (°N)	Longitude (°W)	Altitude (m)	Topographic shielding	Thickness attenuation
NAG01	66 27.777	53 25.913	856	0.9990	0.9581
NAG02	66 27.783	53 25.856	841	1.0000	0.9625
NAG03	66 27.816	53 26.385	755	0.9940	0.9643
NAG04	66 27.809	53 26.116	813	0.9950	0.9678
NAG05	66 27.849	53 26.516	734	0.9970	0.9607
NAG06	66 27.793	53 26.656	574	0.9900	0.9649
NAG07	66 27.819	53 27.219	498	0.9900	0.9586
NAG08	66 27.334	53 25.865	449	0.9880	0.9696
NAG09	66 27.202	53 26.102	359	0.9930	0.9606
NAG10	66 26.990	53 26.613	230	0.9790	0.9609
NAG11	66 27.838	53 29.317	431	0.9980	0.9620
NAG12	66 27.823	53 29.357	409	0.9990	0.9644
NAG14	66 27.759	53 30.185	309	0.9910	0.9612
NAG15	66 27.543	53 30.516	150	0.9790	0.9665
NAG16	66 27.253	53 32.822	339	0.9930	0.9601
NAG17	66 27.291	53 31.846	243	0.9880	0.9610

Table 2. ^{10}Be and ^{26}Al cosmogenic exposure ages for the Nattoralinnguaq valley, detailing production rates and internal and external uncertainties.

Sample code	ID for ^{10}Be AMS	^{10}Be (atoms g^{-1})	sigma ^{10}Be (atoms g^{-1})	Spallogenic site production rate (atoms g^{-1} yr^{-1})	Muogenic Site production rate (atoms g^{-1} yr^{-1})	^{10}Be Exposure age (kyr) no erosion	Internal uncertainty (kyr)	External uncertainty (kyr)	^{10}Be Exposure age (kyr); 10^{-4} cm/a erosion
NAG01	SUERCb2676	$1.408 \cdot 10^{6}$	$3.655 \cdot 10^{4}$	11.82	0.273	**119.8**	3.2	11.1	135.5
NAG02	SUERCb2677	$1.658 \cdot 10^{6}$	$4.621 \cdot 10^{4}$	11.73	0.272	**142.9**	4.1	13.5	161.8
NAG03	SUERCb2678	$6.047 \cdot 10^{5}$	$2.117 \cdot 10^{4}$	10.80	0.264	**55.40**	1.97	5.25	57.92
NAG04	SUERCb2679	$1.160 \cdot 10^{6}$	$3.230 \cdot 10^{4}$	11.44	0.270	**101.4**	2.9	9.5	111.4
NAG05	SUERCb2681	$3.179 \cdot 10^{5}$	$1.118 \cdot 10^{4}$	10.58	0.262	**29.53**	1.05	2.78	30.30
NAG06	SUERCb2796	$1.947 \cdot 10^{5}$	$6.995 \cdot 10^{3}$	9.08	0.248	**21.01**	0.76	1.98	21.37
NAG07	SUERCb2682	$1.747 \cdot 10^{5}$	$6.303 \cdot 10^{3}$	8.38	0.241	**20.39**	0.74	1.92	20.74
NAG08	SUERCb2683	$2.209 \cdot 10^{5}$	$6.414 \cdot 10^{3}$	8.07	0.237	**26.78**	0.78	2.46	27.36
NAG09	SUERCb2687	$1.387 \cdot 10^{5}$	$5.040 \cdot 10^{3}$	7.35	0.229	**18.43**	0.67	1.74	18.71
NAG10	SUERCb3054	$1.066 \cdot 10^{5}$	$3.360 \cdot 10^{3}$	6.35	0.218	**16.30**	0.52	1.51	16.52
NAG11	SUERCb3055	$2.170 \cdot 10^{5}$	$5.857 \cdot 10^{3}$	7.94	0.235	**26.70**	0.73	2.44	27.30
NAG12	SUERCb3056	$1.446 \cdot 10^{5}$	$4.290 \cdot 10^{3}$	7.80	0.233	**18.08**	0.54	1.66	18.33
NAG14	SUERCb3057	$1.069 \cdot 10^{5}$	$3.457 \cdot 10^{3}$	6.97	0.225	**14.90**	0.48	1.38	15.09
NAG15	SUERCb3059	$8.248 \cdot 10^{4}$	$4.721 \cdot 10^{3}$	5.86	0.212	**13.62**	0.78	1.42	13.76
NAG16	SUERCb3060	$7.300 \cdot 10^{4}$	$2.720 \cdot 10^{3}$	7.20	0.227	**9.86**	0.37	0.93	9.94
NAG17	SUERCb3061	$6.903 \cdot 10^{4}$	$2.752 \cdot 10^{3}$	6.49	0.219	**10.31**	0.41	0.99	10.40

Cosmogenic exposure ages ^{26}Al										
Sample code	ID for ^{26}Al AMS	^{26}Al (atoms g^{-1})	sigma ^{26}Al (atoms g^{-1})	Spallogenic site production rate (atoms g^{-1} yr^{-1})	Muogenic site production rate (atoms g^{-1} yr^{-1})	^{26}Al Exposure age (kyr) no erosion	Internal Uncertainty (kyr)	External Uncertainty (kyr)	$^{26}Al/^{10}Be$ (atoms atoms $^{-1}$)	Sigma $Al/^{10}Be$ (atom atoms $^{-1}$)
NAG01	SUERCa751	$8.384 \cdot 10^6$	$2.328 \cdot 10^5$	72.13	2.084	**119.7**	3.5	11.6	5.96	0.23
NAG02	SUERCa752	$9.652 \cdot 10^6$	$2.679 \cdot 10^5$	71.55	2.074	**140.3**	4.2	13.7	5.82	0.23
NAG03	SUERCa753	$3.653 \cdot 10^6$	$1.014 \cdot 10^5$	65.86	2.013	**55.25**	1.57	5.17	6.04	0.27
NAG04	SUERCa754	$6.825 \cdot 10^6$	$1.897 \cdot 10^5$	69.78	2.056	**99.82**	2.92	9.55	5.88	0.23
NAG05	SUERCa756	$2.009 \cdot 10^6$	$6.388 \cdot 10^4$	64.55	1.996	**30.66**	0.99	2.87	6.32	0.30
NAG06	SUERCa757	$1.245 \cdot 10^6$	$4.291 \cdot 10^4$	55.39	1.887	**22.06**	0.77	2.08	6.39	0.32
NAG07	SUERCa758	$1.153 \cdot 10^6$	$4.839 \cdot 10^4$	51.14	1.834	**21.94**	0.93	2.14	6.60	0.37
NAG08	SUERCa762	$1.356 \cdot 10^6$	$4.535 \cdot 10^4$	49.21	1.805	**27.01**	0.91	2.54	6.14	0.27
NAG09	SUERCa764	$9.321 \cdot 10^5$	$4.674 \cdot 10^4$	44.81	1.744	**20.22**	1.02	2.05	6.72	0.39
NAG11	SUERCa822	$1.186 \cdot 10^6$	$5.21 \cdot 10^4$	48.46	1.791	**23.88**	1.06	2.35	5.47	0.28
NAG12	SUERCa823	$8.956 \cdot 10^5$	$4.14. 10^4$	47.58	1.777	**18.31**	0.85	1.82	6.19	0.34